Cell, Volume *133*

Supplemental Data

Identification of Oxidative Stress and Toll-like Receptor 4 Signaling as a Key Pathway of Acute Lung Injury

Yumiko Imai, Keiji Kuba, G. Greg Neely, Rubina Yaghubian-Malhami, Thomas Perkmann, Geert van Lool, Maria Ermolaeva, Ruud Veldhuizen, Y.H. Connie Leung, Hongliang Wang, Haolin Liu, Yang Sun, Manolis Pasparakis, Manfred Kopf, Sina Bavari, J.S. Malik Peiris, Arthur S. Slutsky, Shizuo Akira, Malin Hultqvist, Rikard Holmdahl, John Nicholls, Chengyu Jiang, Christoph J. Binder, and Josef M. Penninger

SUPPLEMENTAL EXPERIMENTAL PROCEDURES

Clinical patient profiles with H5N1 or SARS infection. The two cases of H5N1 infection have been reported previously (Uiprasertkul et al., 2005). Briefly, the first case was a previously healthy 6-year old boy who developed fever and shortness of breath. Despite antibiotic treatment he deteriorated and Chest X-Ray showed right lower lobe opacification. Nasopharyngeal aspirate was positive for influenza A and PCR showed positive result for H5 and negative for H1 and H3. He was started on oseltamivir 2 days before death. The second case was a 33 year old man with previous good health who was admitted with a 4-day history of fever, malaise, sore throat and cough with blood-stained sputum. Chest X-Ray showed right lower-lobe consolidation. Despite treatment with oseltamivir 2 days after admission his condition deteriorated and he developed ARDS. PCR for H5 was positive on day 6 of illness - the day on which he died. The clinical profiles of the nine SARS patients used in our study have been previously reported (Nicholls et al., 2006). Human lung obtained from a patient who died of extra-pulmonary disease served as a normal control and was kindly provided by Prof. D. Kerjaschki, Department of Pathology, Medical University of Vienna, according to ethical guidelines.

Animal infections. For mouse H5N1 infection experiment, female C57BL/6N mice (6-8 week of age) were used. Mice were anesthetized with isoflurane and infected intranasally with live H5N1 avian influenza virus (strain A/HK/483/97) at an equivalent $TCID_{50}$ dose of 10^2 and 10^1. Mice were observed daily and euthanized for tissue sampling on day 4 after challenge. Lung tissues were collected and fixed in 10% formalin. The experiment was conducted in a biosafety level III laboratory. Lethal lung infections with Anthrax, Y. pestis, and monkey pox virus, as well as infections with Smallpox virus, Marburg virus, Western Equine Encephalitis virus (WEE), and Eastern Equine Encephalitis virus (EEE) and lung sampling were performed at the US Army Medical Research Institute of Infectious Diseases, Fort Detrick, according to institutional guidelines. The samples were obtained from USAMRIID's pathology archival collection**.**

Mutant mice. *Tlr4* (Hoshino et al., 1999), *tlr9* (Hemmi et al., 2000), *myd88* (Adachi et al., 1998), *tlr3* (Yamamoto et al., 2003), *trif* (Yamamoto et al., 2003), *irf3* (Sato et al., 2000, *il-6* (Kopf et al., 1994) and *ncf1* (Hultqvist et al., 2004) mutant mice have been previously described. Balb/c, 129Sv, and C57BL/6 mice were bred at our animal facility. C3H/HeJ and C3H/HeOuJ mice were purchased from Jackson laboratories. Of note, the *ncf1* splice mutation was originally identified in the diabetic mouse strains C57BL/6J-m db/db and db/+ (Huang et al., 2000) and backcrossed to the B10.Q backgrounds for more than 12 generations to outcross the diabetic phenotype (Hultqvist et al. 2004). Mice harboring a floxed TRAF6 allele will be reported in detail in the future and were crossed onto LysCre mice (Clausen et al., 1999) to delete TRAF6 in macrophages and neutrophils. Only sex-, age-, and background-matched mice were used as controls. Basal lung function and lung structure were comparable among all the mice tested. Mice were housed in accordance with institutional guidelines.

Acid aspiration-induced acute lung injury model in mice. Mice were anaesthetized with ketamin (75 mg/kg) and xylazine (20 mg/kg) i.p., tracheostomized and ventilated with a volume control constant flow ventilator (Voltek Enterprises, ON, Canada). A volume recruitment maneuver (VRM) (35 cmH_2O, 3 sec) was performed to standardize volume history at baseline. After intratracheal instillation of HCl (pH=1.5; 2 ml/kg), followed by a VRM (35 cmH_2O, 3 seconds), animals were ventilated for 3 hrs (F_IO_2 1.0, and PEEP 2.5 cmH_2O). Saline-treated groups served as controls. Total positive end expiratory pressure ($PEEP_t$) and plateau pressure (P_{plat}) were measured at the end of expiratory and inspiratory occlusion, respectively. Elastance was calculated as (P_{plat} - $PEEP_t$) divided by tidal volume (V_T) every 30 min during the ventilation periods. At the end of the ventilation, left lungs were assessed for lung wet/dry weight ratios or snap frozen in liquid nitrogen for subsequent biochemical analysis. Right lungs were fixed in 10 % buffered formalin for histological examination. To collect BAL fluid for detection of oxidized phospholipids, we performed three washes of 1ml saline each at the end of the 3 hrs ventilation periods.

Bone marrow transplantation. Mouse bone marrow transplantation was performed as described previously (Matute-Bello et al., 2004). In brief, recipient mice were irradiated with 1200 rads. Bone marrow cells from both femurs and tibias were harvested from donor mice under sterile conditions. 50 million nucleated bone marrow cells were obtained from each donor mouse. Bones were flushed with RPMI (Life Technologies, Grand Island, NY) with 10% FCS (Atlanta Biologicals, Norcross, GA). Bone marrow cells were washed twice and counted using a standard hemocytometer. 1 X 10^6 bone marrow cells in 200 µl of media were delivered i.v. through the tail vein of each recipient mouse. Recipient mice were housed in a barrier facility (individually ventilated cages, high energy particulate arresting filter-filtered air), under pathogen-free conditions before and after bone marrow transplantation. Recipient chimeras were used for experiments 12 wks after transplantation.

Preparation of oxidized surfactant phospholipids and *in vivo* treatments. Bovine lipid extract surfactant certified for human patient use was obtained from BLES Biochemicals (London, ON, Canada). *In vitro* oxidation of phospholipids was performed according to previously established conditions and confirmed by electrospray ionization mass spectrometry (Rodriguez Capote et al., 2003). To avoid variable levels of oxidation, this oxidization process was performed on the entire

amount of surfactant required for our studies. The non-oxidized control surfactant PL preparations were from the same production batch as the oxidized material. The purified surfactant PLs we used in our study are certified to be free of LPS and are the material used in patients approved by the FDA. Of note, the endotoxin levels were below the detection limit in both non-oxidized and oxidized surfactant PLs preparations used for our experiments. The *in vivo* impact of non-oxidized surfactant phospholipids (PLs) and oxidized surfactant PLs was tested in normal, healthy lung as well as saline-lavaged lungs to remove surfactant. In both conditions, mice were surgically prepared as described above, and ventilated with a volume control constant flow ventilator (Voltek Enterprises, ON, Canada). Volume recruitment VRM (25 cmH_2O, 3 sec) was performed and measurements were made at baseline. In the normal condition (healthy lungs), either non-oxidized surfactant PLs (50 mg/kg) or oxidized surfactant PLs (50 mg/kg) were instilled intratracheally, followed by a VRM (35 cmH_2O, 3 sec). Animals were then ventilated for 3 hrs (F_IO_2 1.0, and PEEP 2.5 cmH_2O). For removal of endogenous surfactant, lungs were lavaged using a 1-ml syringe filled with 37°C saline (0.15 M NaCl) connected to the endotracheal tube. This procedure was repeated 3 times with 3 min between each lavage followed by a VRM (35 cmH_2O, 3 seconds). Then, animals were treated with either non-oxidized PLs (50 mg/kg body weight) or oxidized PLs (50 mg/kg body weight) intratracheally, followed by a VRM (35 cmH_2O, 3 sec), and ventilated for 3 hrs (F_IO_2 1.0, and PEEP 2.5 cmH_2O).

Polymyxin B, LPS, or OxPAPC treatment in mice *in vivo*. To neutralize LPS, mice received polymyxin B (50 μg, dissolved with 100 μl PBS; Sigma) or control vehicle (100 μl PBS) intratracheally after surgical procedures and were stabilized for 30 min. Animals were then ventilated for 3 hrs and pulmonary elastance was determined as described above. For *in vivo* LPS injection experiment, mice were surgically prepared as above. After intratracheal instillation of either saline**,** HCl (pH 1.5; 2 ml/kg), or LPS (E. coli O111:B4; Sigma Chemical Co., St.Louis, MO*;* 0.5μg/g body weight) followed by a VRM (35 cmH_2O, 3 sec), animals were ventilated for 3 hrs and pulmonary elastance was determined as described above. For *in vivo* OxPAPC treatment, mice were surgically prepared as described above, and OxPAPC (20 μg/g body weight, Avanti Polar Lipids Inc) or control PAPC (20 μg/g body weight, Avanti Polar Lipids Inc) was instilled intratracheally, followed by a VRM (35 cmH_2O, 3 sec). Animals were then ventilated for 3 hrs (F_IO_2 1.0, and PEEP 2.5 cmH_2O) and pulmonary elastance was determined as described above. In addition, we measured the endotoxin levels in the materials used and samples obtained from animals (Limulus Amebocyte Lysate QCL-1000, Cambrex). Endotoxin levels were below detection limits (0.1 EU/ml) in all materials and samples tested including the acid, saline, inactivated H5N1 and H1N1 viruses, surfactant OxPLs, OxPAPC, or PAPC used for our mouse acute lung injury models as well as the BAL fluids obtained from animals before and after induction of ALI following acid or H5N1 challenge.

H5N1 avian influenza isolates, virus inactivation, and H5N1-induced lung injury in mice. Inactivated avian influenza subtypes (H1N1 and A/ck/Yamaguchi/7/04 H5N1) were obtained from the Istituto Zooprofilattico Sperimentale delle Venezie (Padova, Italy). The strain was isolated and characterized according to European guidelines (CEC 92/40). Briefly, virus was inoculated into 9-11 day old SPF embryonated fowl's eggs by the allantoic route. Haemagglutinating allantoic fluid was

collected from eggs and the isolated virus was inactivated using β-propriolactone. Virus inactivation was confirmed by re-inoculation with two blind passages and viruses were serotyped to confirm specific influenza H5N1 subtype. For *in vivo* acute lung injury experiments, mice were surgically prepared and ventilated as described above. VRM (25 cmH_2O, 3 sec) was performed and measurements were made at baseline. Then, 100 μL of either vehicle consisting of allantoic fluid (300 μg protein), inactivated H1N1 viruses (300 μg protein), or inactivated H5N1 viruses (300 μg protein) were instilled intratracheally, followed by a VRM (35 cmH_2O, 3 seconds). Animals were then ventilated for 5 hrs (F_IO_2 1.0, and PEEP 2.5 cmH_2O) and elastance was calculated every 30 min during the ventilation periods. At the end of the ventilation, left lungs were assessed for lung wet/dry weight ratios or snap frozen in liquid nitrogen for subsequent biochemical analysis. Right lungs were fixed in 10 % buffered formalin for histological examination.

Assessment of blood oxygenation and pulmonary edema. Blood samples were obtained from the left ventricle and partial pressure of arterial oxygen (PaO_2) was measured (Ciba-Corning Model 248, Bayer, Leverkusen, Germany) to assess arterial blood oxygenation as an indicator for respiratory failure. To assess pulmonary edemas, the lung wet/dry weight ratios were calculated. In brief, after the blood was drained from excised lungs, measurements of the lung wet weight were made. Lungs were then heated to 65°C in a gravity convection oven for 24 hrs and weighed to determine baseline lung dry mass levels.

Histology, in situ NFκB detection and immunohistochemistry. Lung tissue was fixed in 4% buffered formalin and further processed. For histological analysis, 3-5 μm thick sections were cut and stained with hematoxylin and eosin (H&E). For immunoperoxidase staining to detect phosphorylated NFκBp65 (Vermeulen et al., 2002), paraffin embedded sections were dehydrated, heat pretreated with EDTA buffer CC1 (pH 8.0; 38 min) and incubated with the Ventana Discovery System to expose antigenic epitopes. After blocking endogenous peroxidase activity, sections were incubated with a rabbit polyclonal anti-phospho-NFκBp65 (Ser276) antibody (Cell Signaling; 1:50 dilution) for 60min at room temperature followed by a biotinylated secondary Ab. Biotinylated immune complexes were visualized using a streptavidin-based detection kit. Sections were counter-stained with hematoxylin. Immunohistochemistry to detect oxidized phospholipids (OxPLs) was performed using the mAb EO6 that specifically recognizes the phosphocholine headgroup of OxPLs (Friedman et al., 2002; Horkko et al., 1999). The mAbs EO6 have been described previously (Friedman et al., 2002; Horkko et al., 1999; Palinski et al., 1990) and were kindly provided by Dr. Joseph L. Witztum, La Jolla, USA. Immunohistochemistry for influenza A virus nucleoprotein was performed using the HB 65 (EVL anti-influenza NP, subtype A) antibody as we previously reported (Nicholls et al., 2007).

Multiple cytokine expression analyses and cytokine ELISA. For cytokine protein detection, frozen lung tissues were homogenized in cell lysis buffer, and supernatants were assayed using the Bio-plex multi-plex cytokine array system, which utilizes Luminex-based technology. For the current experiments, a mouse 23-plex assay was used according to recommendations of the manufacturer (BioRad, CA). For ELISA analyses, frozen lung tissues were homogenized in cell lysis buffer, and supernatants were assayed using specific ELISA kits for murine IL-6 (R&D systems, Minneapolis, MN).

Preparation of PAPC/OxPAPC and EO6 binding assay. An adduct of PAPC/oxPAPC with BSA was made as decribed earlier for POVPC-BSA (Bird et al., 1999). Shortly, PAPC or OxPAPC (Avanti Polar Lipids Inc.) was dried under N_2 on borosilicate glass tubes and resuspended with 1 mg/ml BSA/PBS (fatty acid free, MP Biomedicals Inc.) to a final concentration of 2 mM. The mixture was then incubated at 37°C for 4 h, followed by overnight incubation at 37°C after addition of $NaCNBH_3$ (final concentration 10 mM). The preparations were exhaustively dialyzed against PBS to remove unbound PAPC/OxPAPC and $NaCNBH_3$. For EO6 binding assays**,** the BAL samples (adjusted for protein concentration) were applied at different dilutions to 96-well white round-bottomed microtiter plates (ThermoLabsystems, Franklin, MA) and left overnight at 4°C. Plates were then washed four times with PBS/0,27 mM EDTA and blocked with TBS containing 1% BSA for 30. After washing four times with PBS/EDTA, 50µl of EO6 antibody (5µg/ml in TBS/BSA) was added to the wells and incubated for 2 hrs at room temperature. Binding of the EO6 antibody was detected using a goat-anti-mouse IgM-AP labelled antibody (Sigma, St Louis, MO, USA) diluted in TBS/BSA (incubation for 1 h at room temperature), followed by development with 33% LumiPhos Plus solution (Lumigen Inc, Southfield, MI) over 90 min. Light emissions were measured on a WALLAC VIKTOR II luminometer (Perkin Elmer) and expressed as relative light units (RLU)/100 ms.

Isolation and activation of macrophages. Macrophage cultures were grown in RPMI 1640 medium containing 1% FCS, 20 U/ml penicillin, 20 µg/ml streptomycin and 2 mM L-glutamine in an incubator at 37°C with 5% CO_2. Bone marrow cells were isolated from femurs of 8- to 10-week-old mice and cultured for 7 days in medium containing 20 ng/ml recombinant mouse M-CSF (R&D Systems) using bacteriological plastic plates (Bibby Sterilin, Staffordshire, UK). Thioglycollate-elicited peritoneal macrophages were obtained by injecting mice intraperitoneally with 2 ml of 4% thioglycollate broth (Becton Dickinson), followed by peritoneal lavage with 10 ml of PBS 5 days later. Alveolar macrophages were obtained from mice by bronchoalveolar lavage (BAL) with 3 washes of 1 ml PBS and freshly plated for experiments. Lung tissue macrophages were prepared as previously described (Taylor et al., 2006). In brief, lung tissues were excised from mice, finely minced and the tissue pieces placed in medium containing 20 U/ml collagenase and 1 µg/ml DNase. Following incubation, any remaining intact tissue was disrupted by passage through a 40-µm cell strainer (BD Biosciences). The digested cell suspension was then layered on 50% Ficoll, centrifuged at 400g for 40 min and the macrophage layer was collected. Bone marrow, peritoneal, alveolar and lung cells were incubated in 96-well microtitre plates for 2 hrs, and non-adherent cells were removed. For measurement of IL-6, bone marrow macrophages ($1x10^5$ cells), peritoneal macrophages ($1x10^5$ cells), alveolar macrophages ($2x10^4$ cells), or lung macrophages ($1x10^5$ cells) were plated on 96-well plates and stimulated *in vitro*. For OxPAPC or PAPC stimulation experiment, cells were treated with BSA-conjugated OxPAPC or BSA-conjugated PAPC as described above for 24 hrs. In some experiments an isotype matched control Ab (mouse IgM) and the IgM mAb EO6 were added to the macrophage cultures at a final concentration of 10 µg/ml. IL-6 levels in supernatants were assayed in triplicate cultures after 24 hrs of stimulation using specific ELISA kits for murine IL-6 (R&D systems).

Detection of ROS and TLR4 on mouse alveolar macrophages by FACS. Alveolar macrophages were obtained by bronchoalveolar lavage (BAL) with 3 washes of 1 ml PBS from mice one hour after control, acid, or inactivated H5N1 treatment as described above. For ROS detection, cells were

washed twice in HBSS, and then resuspended in 200 μl HBSS (14060-040, Gibco) and incubated at 37ºC for 30 minutes in the presence of DCF (I36007, Invitrogen). For TLR4 cell surface expression, cells were pretreated with Fc blocking agents (antiCD16/CD32, 553142, Pharmingen) and stained for CD11c-APC (550261, Pharmingen) and TLR-4-PE (12-9041-80, eBioscience), washed twice and assessed by FACS (FACScalibur, BD).

Western blotting. Lung tissues were homogenized in ice-cold lysis buffer (50 mM Tris-HCl, pH 7.5, 150 mM NaCl, 1.0% Triton X-100, 20 mM EDTA, 1 mM Na_3VO_4, 1 mM NaF and protease inhibitors). Tissue lysates were separated by SDS-PAGE and proteins were transferred onto polyvinyldifluoride membranes. Membranes were incubated with antibodies to rabbit polyclonal human IκBα (Cell signaling) and β-actin followed by horseradish peroxidase–conjugated secondary antibodies. Binding was visualized using the ECL detection system (Amersham Pharmacia).

Measurement of ROS and TLR4 in human peripheral blood monocytes (PBMC). Human PBMC were isolated as previously described with Ficoll-Hypaque (TBDscience). For the inactivated H5N1 and H1N1 virus experiments, monocytes were treated with inactivated H5N1 virus or H1N1 virus as described above for 6 hours at 37°C. For ROS detection, cells were washed twice in HBSS, and then resuspended in 200 μl HBSS (14060-040, Gibco) and incubated at 37ºC for 30 minutes in the presence of DCF (I36007, Invitrogen). For TLR4 cell surface expression, cells were stained for anti-TLR4 (Santa Cruz Biotechology), washed twice and assessed by FACS (FACScalibur, BD). PC5-CD14 staining was used to gate the monocyte population.

Indirect immunofluorescence microscopy for TLR4 localization. Human PBMCs were isolated as described above. Cells were then mock treated with aluminum adjuvant (control) or 40μl H5N1 vaccine (kind gift of Qian Yuan Hao, Zhenzhou Bio-pharmaceutical factory) for 6 hours at 37°C. Cells were then fixed with 4% paraformaldehyde in PBS, permeabilized with 0.1% Triton-X100 in PBS, incubated in blocking buffer (3% BSA in PBS), then incubated with anti-TLR4 (Santa Cruz Biotechology, 1:200 dilution) diluted in blocking buffer. Primary antibody binding was detected with Alexa Fluor 488 goat anti-rabbit IgG (Molecular Probes, 1:200 dilution). Cells were then washed three times with PBS and mounted on glass slides. Images were obtained with a Leica confocal microscope. TLR4 surface expression was confirmed as described above for murine macrophages.

Statistical analyses. All data are shown as mean ± s.e.m.. Measurements at single time points were analyzed by ANOVA and if significant, further analyzed by a two-tailed t-test. Time courses were analyzed by repeated measurements (mixed model) ANOVA with Bonferroni post-tests. All statistical tests were calculated using the GraphPad Prism 4.00 (GraphPad Software, San Diego, CA, USA). $P < 0.05$ was considered to indicate statistical significance.

SUPPLEMENTAL REFERENCES

Adachi, O., Kawai, T., Takeda, K., Matsumoto, M., Tsutsui, H., Sakagami, M., Nakanishi, K., and Akira, S. (1998). Targeted disruption of the MyD88 gene results in loss of IL-1- and IL-18-mediated function. Immunity *9*, 143-150.

Bird, D. A., Gillotte, K. L., Horkko, S., Friedman, P., Dennis, E. A., Witztum, J. L., and Steinberg, D. (1999). Receptors for oxidized low-density lipoprotein on elicited mouse peritoneal macrophages can recognize both the modified lipid moieties and the modified protein moieties: implications with respect to macrophage recognition of apoptotic cells. Proc Natl Acad Sci U S A *96*, 6347-6352.

Bueno, R., Mello, M. N., Menezes, C. A., Dutra, W. O., and Santos, R. L. (2005). Phenotypic, functional, and quantitative characterization of canine peripheral blood monocyte-derived macrophages. Mem Inst Oswaldo Cruz *100*, 521-524.

Clausen, B. E., Burkhardt, C., Reith, W., Renkawitz, R., and Forster, I. (1999). Conditional gene targeting in macrophages and granulocytes using LysMcre mice. Transgenic Res *8*, 265-277.

Friedman, P., Horkko, S., Steinberg, D., Witztum, J. L., and Dennis, E. A. (2002). Correlation of antiphospholipid antibody recognition with the structure of synthetic oxidized phospholipids. Importance of Schiff base formation and aldol concentration. J Biol Chem *277*, 7010-7020.

Hemmi, H., Takeuchi, O., Kawai, T., Kaisho, T., Sato, S., Sanjo, H., Matsumoto, M., Hoshino, K., Wagner, H., Takeda, K., and Akira, S. (2000). A Toll-like receptor recognizes bacterial DNA. Nature *408*, 740-745.

Horkko, S., Bird, D. A., Miller, E., Itabe, H., Leitinger, N., Subbanagounder, G., Berliner, J. A., Friedman, P., Dennis, E. A., Curtiss, L. K., *et al.* (1999). Monoclonal autoantibodies specific for oxidized phospholipids or oxidized phospholipid-protein adducts inhibit macrophage uptake of oxidized low-density lipoproteins. J Clin Invest *103*, 117-128.

Hoshino, K., Takeuchi, O., Kawai, T., Sanjo, H., Ogawa, T., Takeda, Y., Takeda, K., and Akira, S. (1999). Cutting edge: Toll-like receptor 4 (TLR4)-deficient mice are hyporesponsive to lipopolysaccharide: evidence for TLR4 as the Lps gene product. J Immunol *162*, 3749-3752.

Hultqvist, M., Olofsson, P., Holmberg, J., Backstrom, B. T., Tordsson, J., and Holmdahl, R. (2004). Enhanced autoimmunity, arthritis, and encephalomyelitis in mice with a reduced oxidative burst due to a mutation in the Ncf1 gene. Proc Natl Acad Sci U S A *101*, 12646-12651.

Kopf, M., Baumann, H., Freer, G., Freudenberg, M., Lamers, M., Kishimoto, T., Zinkernagel, R., Bluethmann, H., and Kohler, G. (1994). Impaired immune and acute-phase responses in interleukin-6-deficient mice. Nature *368*, 339-342.

Matute-Bello, G., Lee, J. S., Frevert, C. W., Liles, W. C., Sutlief, S., Ballman, K., Wong, V., Selk, A., and Martin, T. R. (2004). Optimal timing to repopulation of resident alveolar macrophages with donor cells following total body irradiation and bone marrow transplantation in mice. J Immunol Methods *292*, 25-34.

Nicholls, J. M., Butany, J., Poon, L. L., Chan, K. H., Beh, S. L., Poutanen, S., Peiris, J. S., and Wong, M. (2006). Time course and cellular localization of SARS-CoV nucleoprotein and RNA in lungs from fatal cases of SARS. PLoS Med *3*, e27.

Nicholls, J. M., Chan, M. C., Chan, W. Y., Wong, H. K., Cheung, C. Y., Kwong, D. L., Wong, M. P., Chui, W. H., Poon, L. L., Tsao, S. W., *et al.* (2007). Tropism of avian influenza A (H5N1) in the upper and lower respiratory tract. Nat Med *13*, 147-149.

Palinski, W., Yla-Herttuala, S., Rosenfeld, M. E., Butler, S. W., Socher, S. A., Parthasarathy, S., Curtiss, L. K., and Witztum, J. L. (1990). Antisera and monoclonal antibodies specific for epitopes generated during oxidative modification of low density lipoprotein. Arteriosclerosis *10*, 325-335.

Rodriguez Capote, K., McCormack, F. X., and Possmayer, F. (2003). Pulmonary surfactant protein A (SP-A) restores the surface properties of surfactant after oxidation by a mechanism that requires the Cys6 interchain disulfide bond and the phospholipid binding domain. J Biol Chem *278*, 20461-20474.

Sato, M., Suemori, H., Hata, N., Asagiri, M., Ogasawara, K., Nakao, K., Nakaya, T., Katsuki, M., Noguchi, S., Tanaka, N., and Taniguchi, T. (2000). Distinct and essential roles of transcription factors IRF-3 and IRF-7 in response to viruses for IFN-alpha/beta gene induction. Immunity *13*, 539-548.

Taylor, J. L., Hattle, J. M., Dreitz, S. A., Troudt, J. M., Izzo, L. S., Basaraba, R. J., Orme, I. M., Matrisian, L. M., and Izzo, A. A. (2006). Role for matrix metalloproteinase 9 in granuloma formation during pulmonary Mycobacterium tuberculosis infection. Infect Immun *74*, 6135-6144.

Uiprasertkul, M., Puthavathana, P., Sangsiriwut, K., Pooruk, P., Srisook, K., Peiris, M., Nicholls, J. M., Chokephaibulkit, K., Vanprapar, N., and Auewarakul, P. (2005). Influenza A H5N1 replication sites in humans. Emerg Infect Dis *11*, 1036-1041.

Vermeulen, L., De Wilde, G., Notebaert, S., Vanden Berghe, W., and Haegeman, G. (2002). Regulation of the transcriptional activity of the nuclear factor-kappaB p65 subunit. Biochem Pharmacol *64*, 963-970.

Yamamoto, M., Sato, S., Hemmi, H., Hoshino, K., Kaisho, T., Sanjo, H., Takeuchi, O., Sugiyama, M., Okabe, M., Takeda, K., and Akira, S. (2003). Role of adaptor TRIF in the MyD88-independent toll-like receptor signaling pathway. Science *301*, 640-643.

Figure S1. C3H/HeJ mice are resistant to acid aspiration-induced acute lung injury

A, Changes in lung elastance in defined mouse inbred strains (C57BL/6, Balb/c, 129Sv, C3H/HeOuJ and C3H/HeJ) in response to acid injury. C3H/HeJ mice exhibited markedly improved lung elastance compared to other mouse strains. ** $P < 0.01$ for the whole time course comparing C57BL/6, Balb/c, C3H/HeOuJ, or 129Sv mice. n = 6-10 for each group. **B,** Partial pressure of oxygen in arterial blood (PaO_2 in mmHg) after saline or acid treatment in C3H/HeOuJ and C3H/HeJ mice. n = 5-6 for acid-treated groups, n = 4 for saline-treated groups. * $P < 0.05$. **C,** Lung histopathology in acid-treated C57BL/6, Balb/c, C3H/HeJ, and C3H/HeOuJ mice. Note reduced hyaline membrane formation, inflammatory cell infiltration, and bleeding in acid-treated C3H/HeJ mice. H&E staining. Original magnifications X 200. Lungs were analyzed 3 hrs after treatment. **D,** Changes in lung elastance after acid or saline treatment in TLR4-congenic C3H/HeOuJ and C3H/HeJ mice. n = 6 for acid-treated groups, n = 4 for saline-treated groups. ** $P < 0.01$ for the whole time course comparing acid-treated C3H/HeJ and C3H/HeOuJ mice. Data in **A, B** and **D** are shown as mean values +/- s.e.m..

Figure S2. Acid aspiration-induced acute lung injury is independent of TLR3, TLR9, or IRF3 expression

A, Lung elastance after acid treatment in wild type (WT), toll like-receptor 9 knock-out (*tlr9*$^{-/-}$), and toll like-receptor 3 knock-out (*tlr3*$^{-/-}$) mice. n = 6-10 for each group. **B**, Wet-to-dry ratios of lungs 3 hrs after acid injury in WT, *tlr9*$^{-/-}$, and *tlr3*$^{-/-}$ mice. In **A** and **B**, there were no significant differences among the groups. **C**, Lung elastance after acid treatment in WT and MyD88 knock-out (*myd88*$^{-/-}$) mice. n = 6-10 for each group. **D,** Wet-to-dry weight ratios of lungs 3 hrs after acid injury in WT and *myd88*$^{-/-}$ mice. In **C** and **D**, there were no significant statistical differences between the groups. **E**, Changes in lung elastance following acid treatment in interferon-regulatory factor 3 mutant (*irf3*$^{-/-}$) and control WT mice. n = 6-10 each group. **F,** Wet-to-dry ratios of lungs 3 hrs after acid treatment in *irf3*$^{-/-}$ and control WT mice. n = 6-10 for each group. In **E** and **F**, there were no significant statistical differences between the experimental groups. All data are shown as mean values +/- s.e.m..

Figure S3. Lung edema formation in *trif*$^{-/-}$, TRAF6$^{MC\text{-}KO}$, and *il-6*$^{-/-}$ mice

A, Lung edema formation (wet-to-dry ratios) 3 hrs after acid or saline aspiration in WT and *trif*$^{-/-}$ mice.

* $P < 0.05$. **B,** Wet-to-dry weight ratios of lungs 3 hrs after acid treatment in TRAF6$^{MC\text{-}WT}$ and TRAF6$^{MC\text{-}KO}$ mice. * $P < 0.05$. **C,** Loss of IL-6 results in improved edema formation. Wet-to-dry weight ratios of lungs 3 hrs after acid treatment in WT and *il-6*$^{-/-}$ mice are shown. n = 5-6 for each group. * $P < 0.05$.

All data are shown as mean values +/- s.e.m..

Figure S4. Cytokine profiles in acid-treated lung

IL-1β (**A**), KC (**B**), TNFα (**C**), IL-2 (**D**), and IL-10 (**E**) levels in lungs of wild type control and the indicated mutant mouse strains following acid treatment. Since there were no differences in the cytokine levels among acid treated wild type control mice (Balb/c, BL6, and TRAF6 $^{MC\text{-}WT}$) only data from Balb/c mice are shown as the acid-treated WT group. Note that IL-10 levels were significantly increased in acid treated *tlr4*$^{-/-}$, *trif*$^{-/-}$, and TRAF6$^{MC\text{-}KO}$, but not *myd88*$^{-/-}$ and *ifr3*$^{-/-}$ mice. *P < 0.05, compared to WT. *n* = 6-10 for each group. All data are shown as mean values +/- s.e.m..

Figure S5. LPS neutralization and injection, and generation of malondialdehyde epitopes

A, Changes in lung elastance in wild type mice treated with vehicle or polymyxin B (50μg) after acid instillation. *n* = 6 for each group. Data are shown as mean values +/- s.e.m.. **B**, Changes in lung elastance in wild type (WT) mice treated with saline, LPS, or acid. *n* = 5 for each group. ** *P* < 0.01 for the whole time course comparing acid- and LPS-treated mice. **C,** Detection of EO6-detectable OxPLs in the bronchoalveolar lavage (BAL) of control mice and mice 3 hrs after acid aspiration. Y-axis shows *in vitro* binding to the mAb EO6 in relative light units (RLU). n=3 each group. ** *P* < 0.01 comparing to BAL fluid of control mice. **D,** Immunohistochemistry for malondialdehyde epitopes detected by the mAb MDA2 in lungs of saline-treated control and acid treated wild type (WT) mice. Malondialdehyde epitopes were localized to inflammatory exudates lining the injured alveoli (arrows) in acid-treated lungs. Original magnifications X 400. Data in **A, B** and **C** are shown as mean values +/- s.e.m..

Figure S6. Oxidized phospholipids from injured lungs can trigger IL-6 production via TLR4.

A,B Bronchoalveolar lavage (BAL) fluid obtained from mice following acid aspiration (BAL acid) induces large amounts of interleukin-6 (IL-6) in wild type (WT), but not *tlr4*$^{-/-}$ **(A)** peritoneal and **(B)** bone marrow macrophages. Incubation of macrophages with BAL fluid obtained from healthy WT mice is shown as a control (BAL control). BAL fluids containing an isotype matched mouse IgM control Ab were compared to BAL fluids plus the mAb EO6. **C,** Lung immunohistochemistry for OxPLs detected by the mAb EO6 in *tlr4*$^{-/-}$ mice 3 hrs after acid aspiration. OxPLs localize to inflammatory exudates lining the injured alveoli (arrow) as well as macrophages (arrowhead). Original magnifications X 400. **D**, Binding curves of the mAb EO6 to oxidized or non-oxidized surfactant PLs confirming the presence of EO6-detectable phospholipids in surfactant..Y-axis shows *in vitro* binding to the mAb EO6 in relative light units (RLU). Data in **A, B** and **D** are shown as mean values +/- s.e.m..

Figure S7. Oxidized phospholipids induce acute lung injury *in vivo* and structure of 1-palmitoyl-2-arachidonoyl-phosphatidylcholine (PAPC).

A, Lung elastance in mice that received saline lung lavage followed by an intratracheal replacement with non-oxidized or oxidized surfactant PLs. n = 3-4 for each group. Following a challenge with oxidized surfactant PLs, all animals died during the experiment, whereas mice that received non-oxidized PLs stabilized their lung function. ** $P < 0.01$ comparing non-oxidized PLs. **B,** IL-6 levels in lung tissue of control WT and *tlr4*$^{-/-}$ mice following administration of non-oxidized PLs or oxidized PLs. ** $P < 0.01$ comparing oxidized PLs treated *tlr4*$^{-/-}$ mice. **C**, Bioactive products of PAPC are formed by oxidative modification, in which the sn2-fatty acid is either fragmented or modified by addition of oxygens. The PC head group in these products is retained and now available for recognition by the IgM Ab EO6. Any double bond in the unsaturated fatty acid (sn2) of the PAPC is a site where oxidation occurs (arrowhead points at one such bond). Data in **A** and **B** are shown as mean values +/- s.e.m..

Figure S8. Oxidized PAPC induces pulmonary IL-6 production via TLR4

A, Binding of BSA-conjugated OxPAPC with mAbEO6. Y-axis shows *in vitro* binding to the mAb EO6 in relative light units (RLU). **B**, Increase in IL-6 production from baseline (unstimulated control, con) in alveolar macrophages isolated from wild type (WT) mice in response to PAPC or OxPAPC in the presence of an isotype matched control mAb or the mAb EO6. *$P < 0.05$ comparing mAb EO6. [a]**$P < 0.01$ comparing 1.0μg/ml OxPAPC EO6(-). [b]**$P < 0.01$ comparing 10.0μg/ml OxPAPC EO6(-). Data are from 4 separate experiments. **C**, Increase in IL-6 production from baseline (unstimulated control, con) in alveolar macrophages isolated from WT control and *tlr4*$^{-/-}$ mice in response to LPS (1ng/ml) or OxPAPC (10μg/ml). *$P < 0.05$ comparing OxPAPC treated WT macrophages in the presence or absence of EO6. **$P < 0.01$ comparing OxPAPC EO6(-) treated WT macrophages with OxPAPC EO6(-) treated *tlr4*$^{-/-}$ macrophages. Data are from 4 separate experiments. **D**, Increase in IL-6 production from baseline (unstimulated control, con) in peritoneal macrophages isolated from WT control, *tlr4*$^{-/-}$, *myd88*$^{-/-}$, and *trif*$^{-/-}$ mice in response to LPS (1ng/ml) or OxPAPC (10μg/ml). **$P < 0.01$ comparing OxPAPC EO6(-) treated WT macrophages. Data are from 3 separate experiments. **E**, IL-6 levels in lung tissue of control WT, *tlr4*$^{-/-}$, *myd88*$^{-/-}$, and *trif*$^{-/-}$ mice following administration of OxPAPC. The genetic backgrounds are indicated. The WT shown in D, is from a BL6 background. n = 4 each group. *$P < 0.05$. All data are shown as mean values +/- s.e.m..

Figure S9. Histology and oxidized phospholipids formation of lungs treated with inactivated H5N1 virus

A, Lung pathology (H&E staining) in lung tissue of vehicle treated or H5N1 and H1N1 challenged WT mice. Challenge with the inactivated H5N1 virus results in markedly increased inflammatory cell infiltration, bleeding, and hyaline membrane formation. Data are at 5 hrs after challenge. Original magnifications X 400. **B,** Detection of OxPLs in the bronchoalveolar lavage (BAL) fluid of vehicle and inactivated H5N1 treated WT mice. Y-axis shows *in vitro* binding to mAb EO6 in relative light units (RLU). n = 3 each group. ** $P < 0.01$. **C**, OxPLs in lungs from vehicle treated control mice and

mice challenged with inactivated H5N1 viruses detected by the mAb EO6. Lungs were analyzed 5 hrs after treatment. The H5N1 challenge results in the generation of OxPLs in inflammatory exudates lining the injured air spaces (arrows). Original magnifications X 400. **D**, Lung edema formation (wet to dry weight ratios) in control WT versus versus *trif*$^{-/-}$ mice 5 hrs after challenge with inactivated H5N1 viruses. ** $P < 0.01$. Data in **B** and **D** are shown as mean values +/- s.e.m..

Figure S10. Absence of EO6-detectable OxPLs in lungs from control patients

A, TLR4 surface expression in CD14^{+} gated control human PBMCs or PMBCs treated for 3 hrs with inactivated H5N1 or H1N1 viruses. * $P < 0.05$. Data are shown as mean values (+/- s.e.m.) from 6 different healthy donors. **B,** Lung edema formation (wet to dry weight ratios) in control WT versus *ncf1* mutantmice 5 hrs after challenge with inactivated H5N1 viruses. ** $P < 0.01$. **C**, Absence of EO6-detectable OxPLs in lungs from two different control patients. Lungs were immunostained with the mAb EO6 as described above. Original magnifications X 400.

Figure S11. Proposed lung injury pathway involved in the disease pathogenesis of ARDS.

The scheme is based on genetic and functional analysis reported in this paper. See discussion for details.

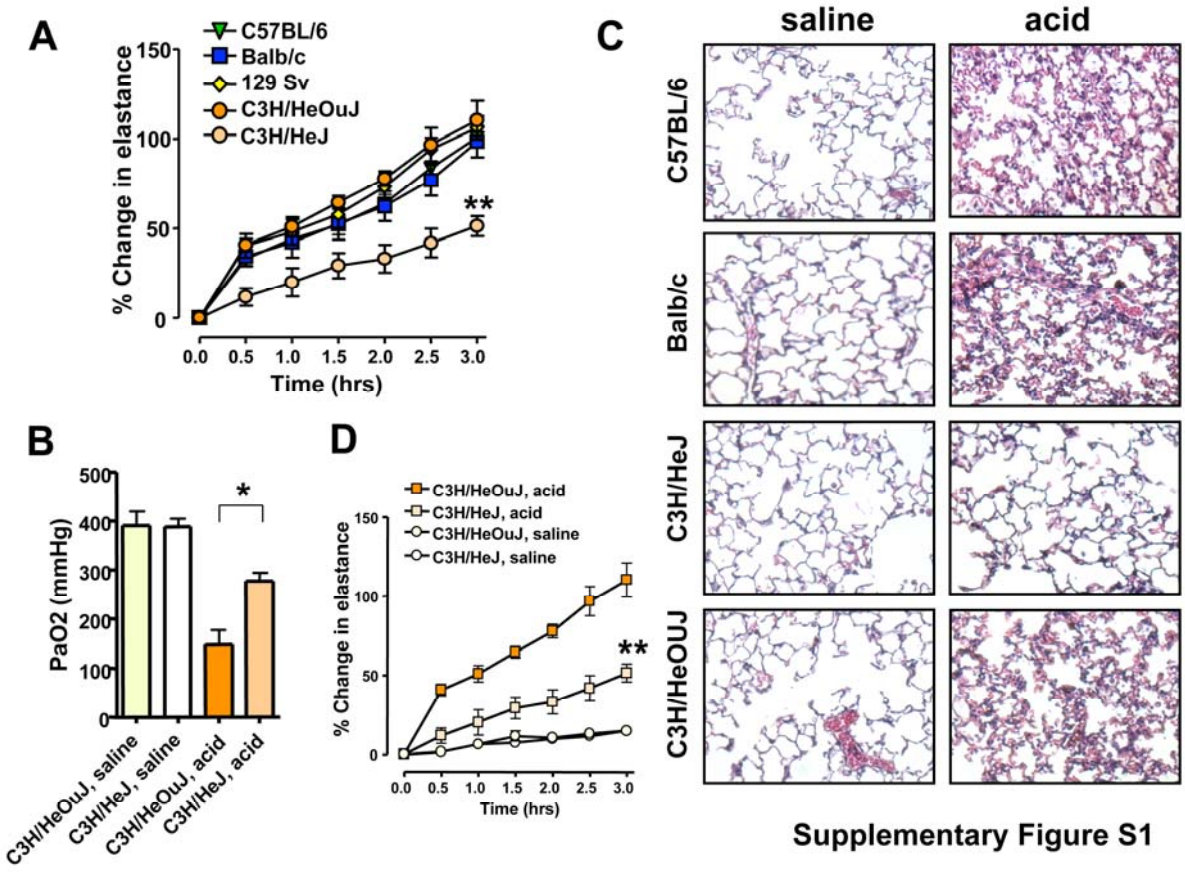

Supplementary Figure S1

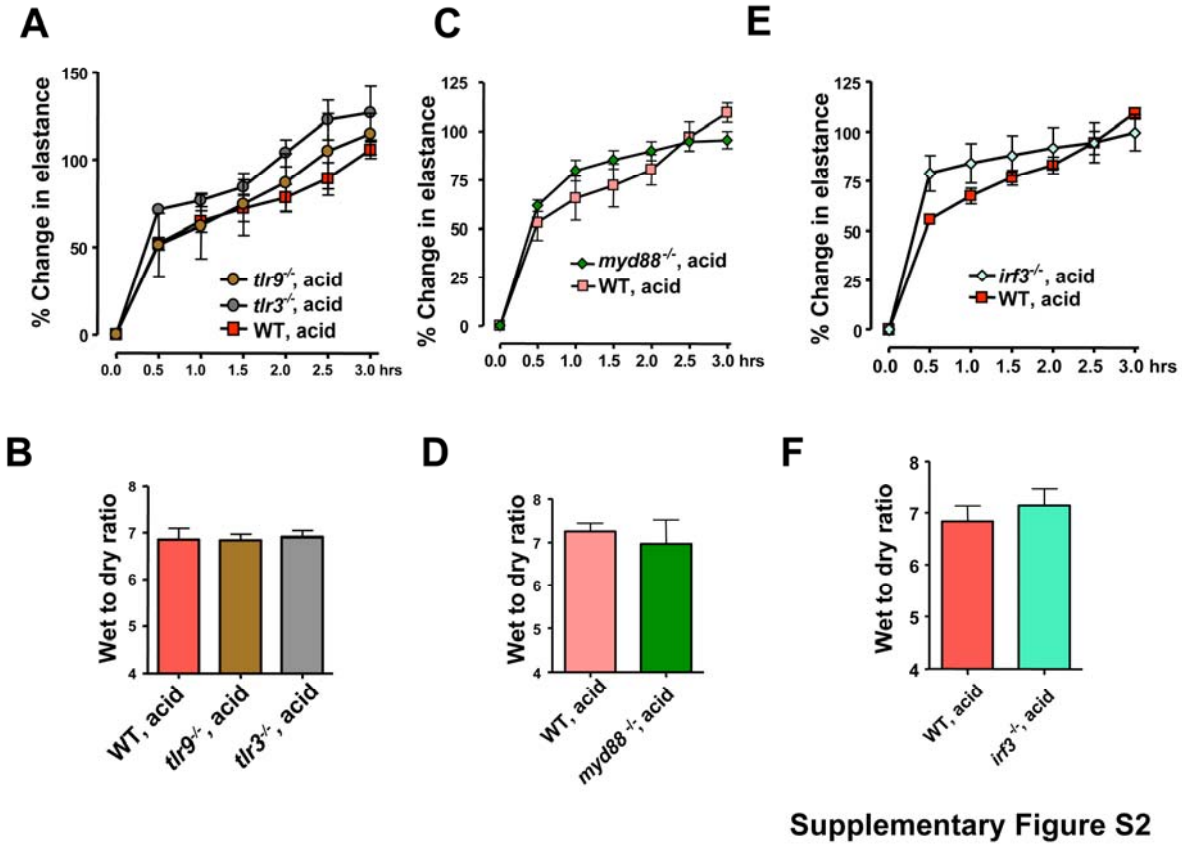

Supplementary Figure S2

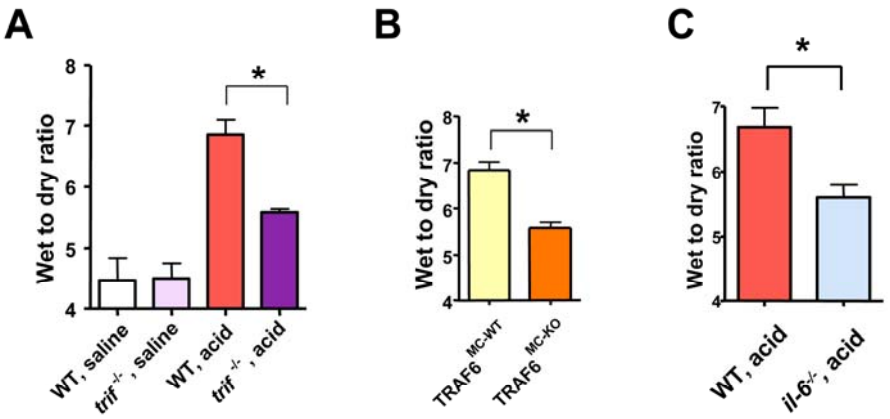

Supplementary Figure S3

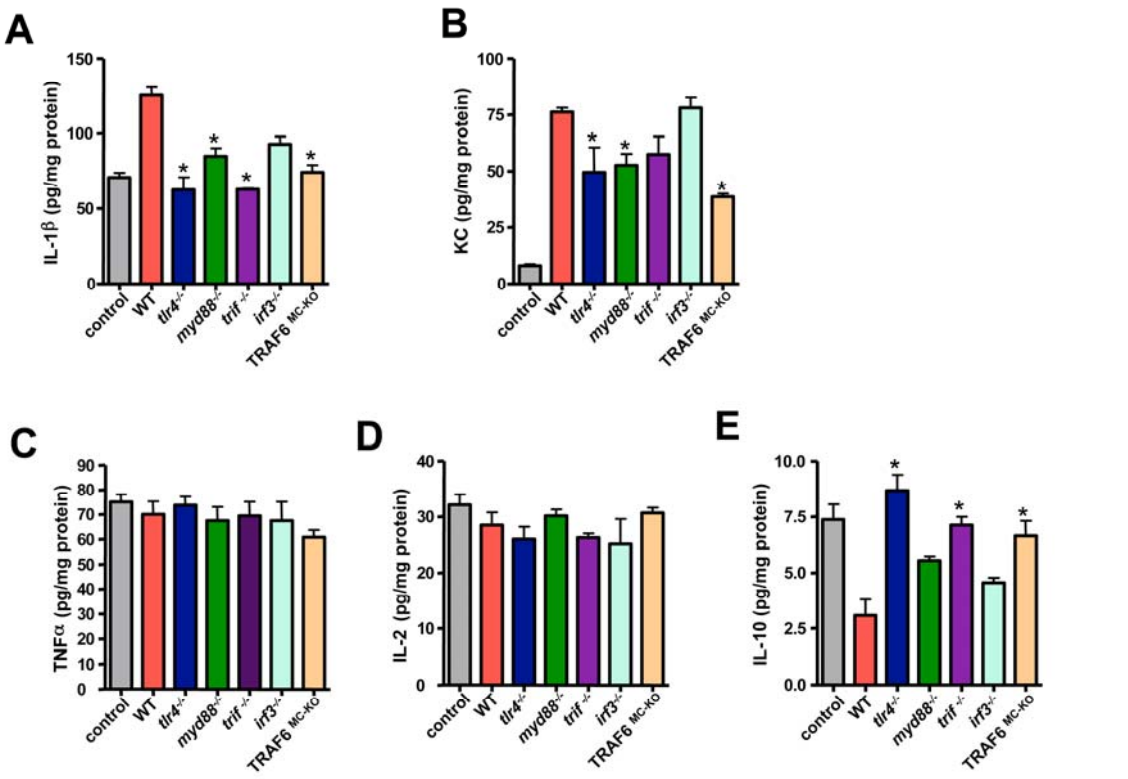

Supplementary Figure S4

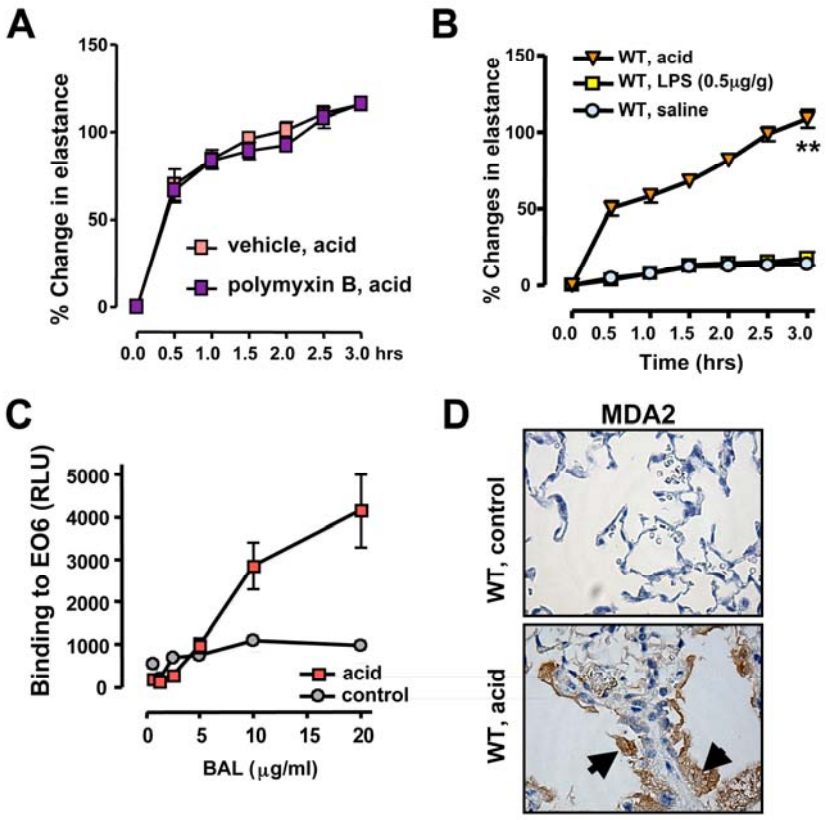

Supplementary Figure S5

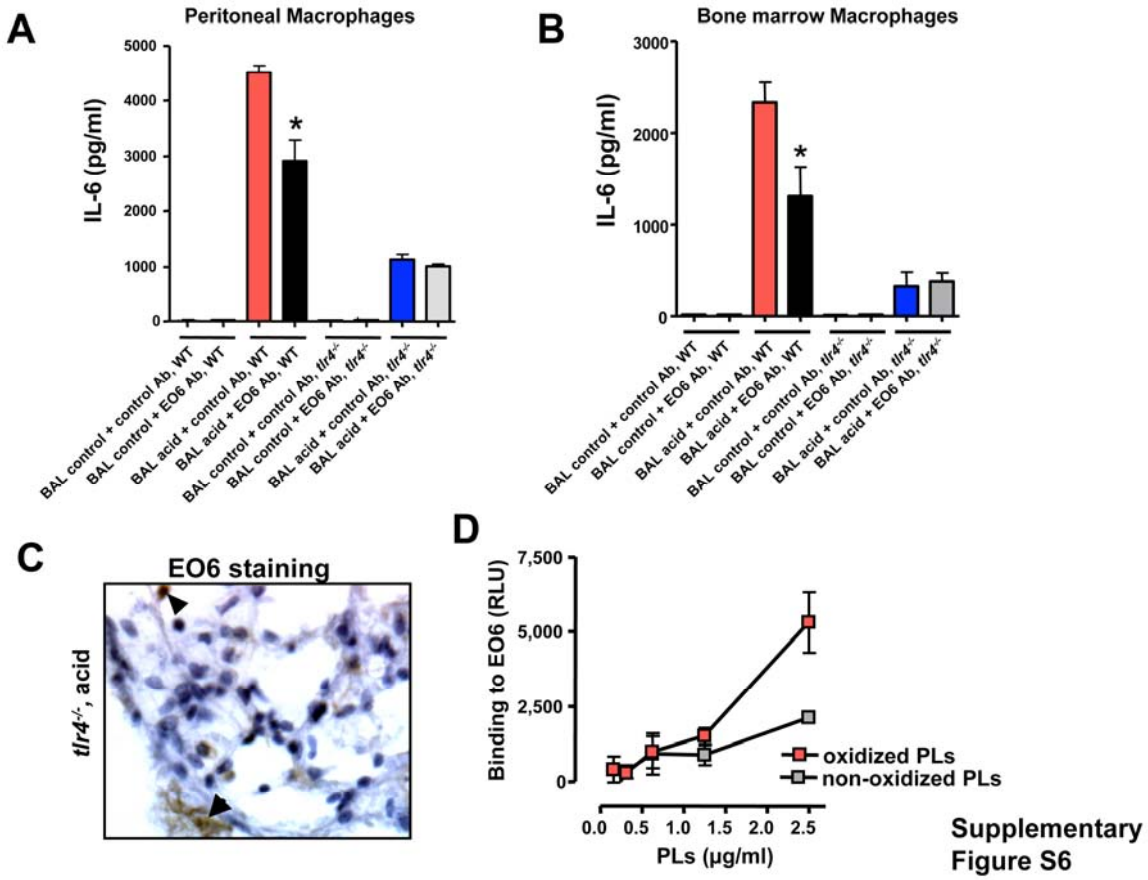

Supplementary Figure S6

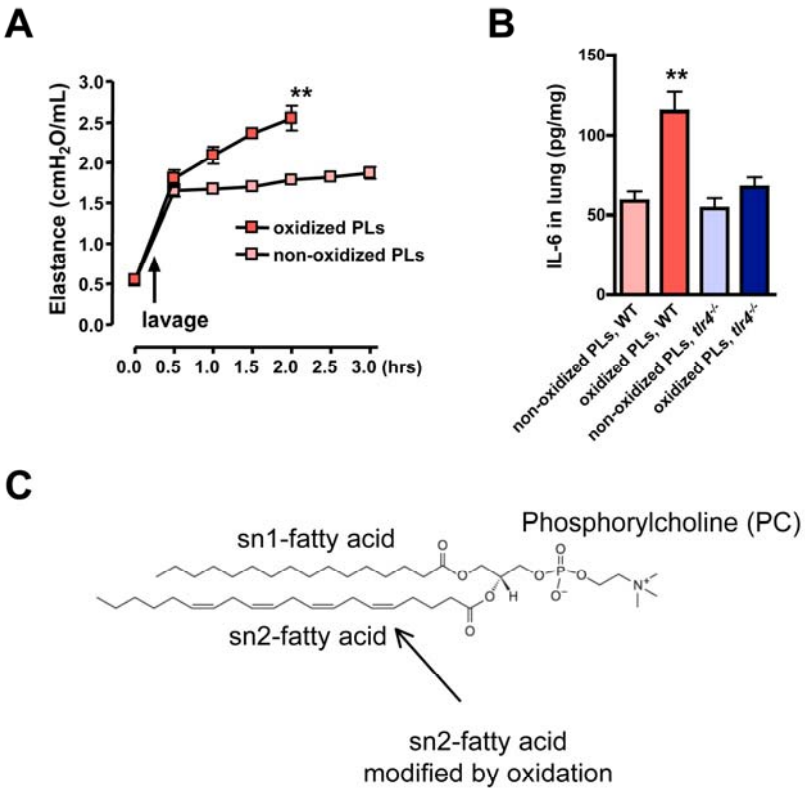

Supplementary Figure S7

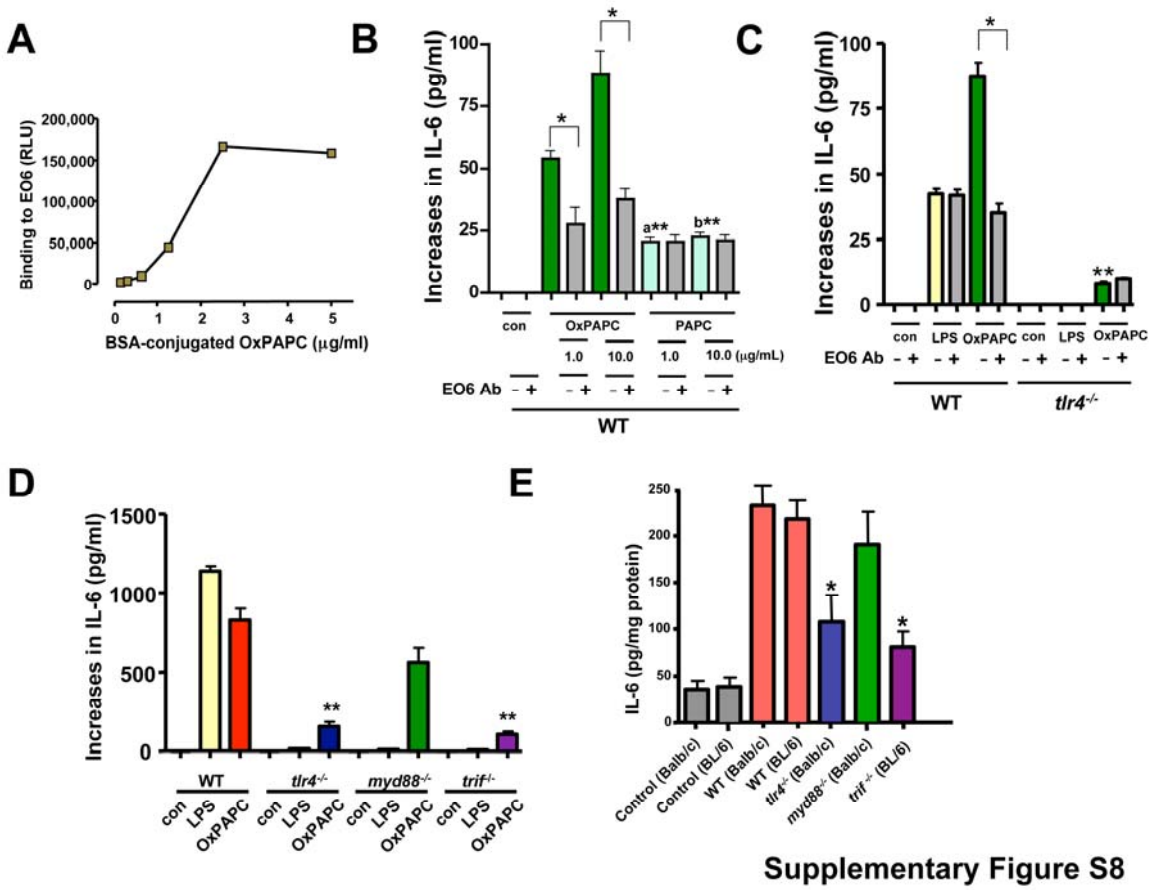

Supplementary Figure S8

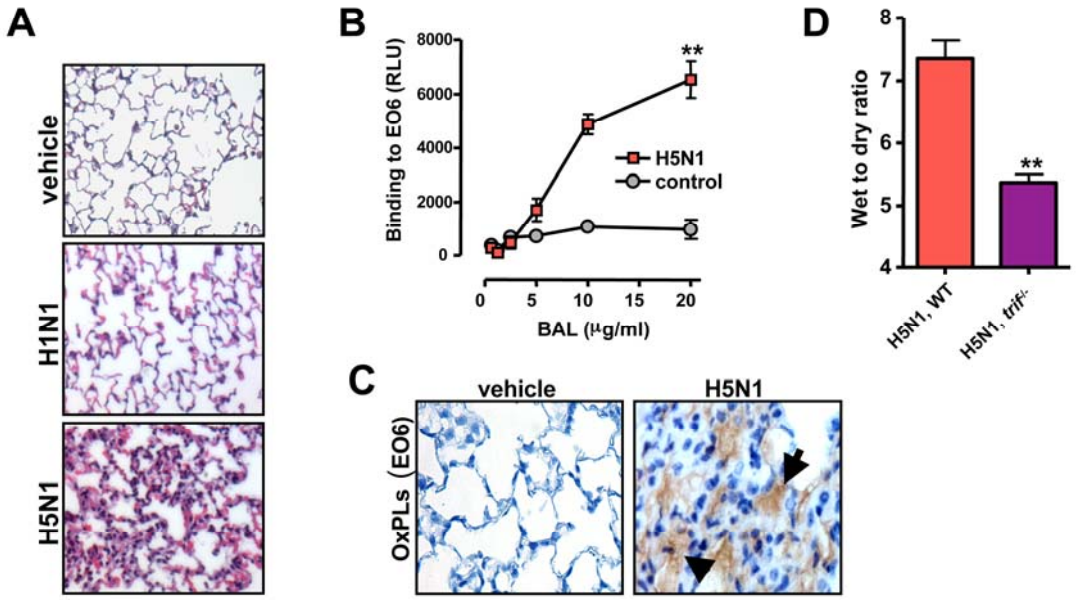

Supplementary Figure S9

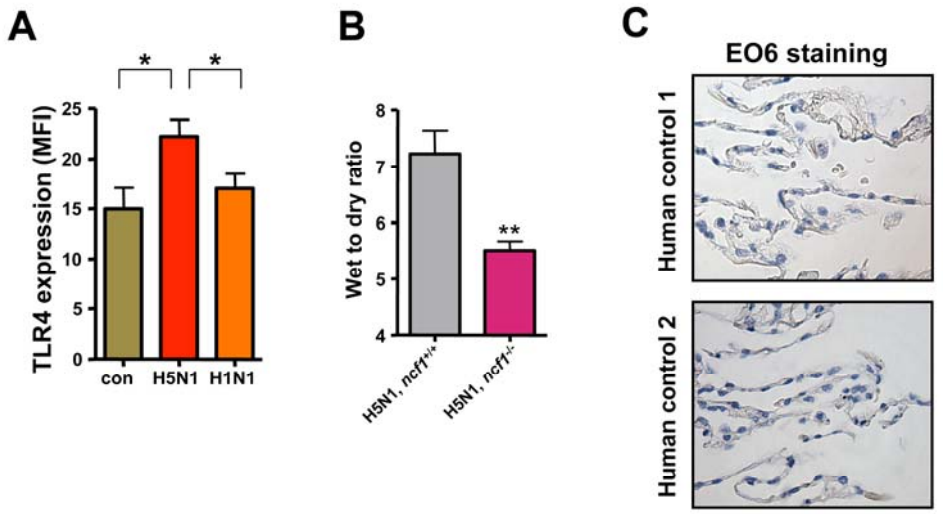

Supplementary Figure S10

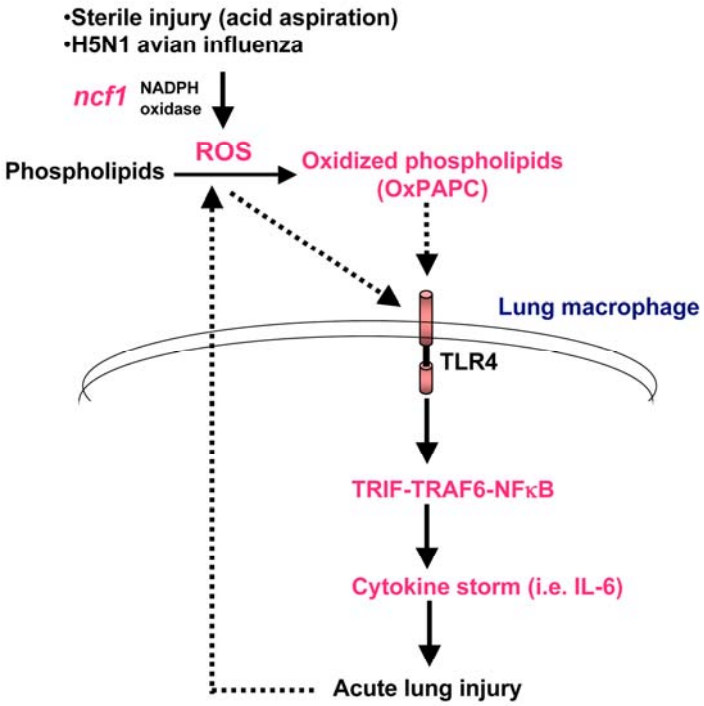

Supplementary Figure S11